Chinese Chemical Letters 33 (2022) 3534–3538

Contents lists available at ScienceDirect

Chinese Chemical Letters

journal homepage: www.elsevier.com/locate/cclet

# Epoxy-POSS/silicone rubber nanocomposites with excellent thermal stability and radiation resistance

Mengni Shi[a,1], Yinyong Ao[b,1], Lei Yu[b], Lang Sheng[a], Shuangxiao Li[a], Jing Peng[a], Hongbing Chen[b], Wei Huang[b], Jiuqiang Li[a], Maolin Zhai[a,*]

[a] Beijing National Laboratory for Molecular Sciences, Radio Chemistry and Radiation Chemistry Key Laboratory of Fundamental Science, The Key Laboratory of Polymer Chemistry and Physics of the Ministry of Education, College of Chemistry and Molecular Engineering, Peking University, Beijing 100871, China
[b] Institute of Nuclear Physics and Chemistry, China Academy of Engineering Physics, Mianyang 621900, China

ARTICLE INFO

*Article history:*
Received 26 November 2021
Revised 15 March 2022
Accepted 15 March 2022
Available online 18 March 2022

*Keywords:*
POSS
Silicone rubber
Thermal stability
Radiation resistance
Radiation crosslinking and degradation mechanism

ABSTRACT

Due to the rigid Si-O-Si backbone, silicone rubber (SR) have a widespread application in extreme environment such as high temperature and high-level radiation. However, the radiation stability of SR still does not meet the practical needs in special radiation environments. Herein we prepared epoxy POSS(ePOSS)/SR nanocomposites with excellent thermal stability and radiation resistance. As a physical crosslinking point in the SR, addition of small amount of ePOSS not only enhanced the mechanical properties of the matrix, but also improved its thermal stability greatly due to their good compatibility. ePOSS/SR had higher radiation stability in air than SR owing to the inhibition of radiation oxidation by ePOSS, and the yield of main gaseous radiolysis products ($CH_4$, $H_2$, CO and $CO_2$) of SR and ePOSS/SR nanocomposites was determined. By analyzing the changes of chemical structure, thermal properties and mechanical properties of the ePOSS/SR nanocomposite, combined with the characteristics of gas products after $\gamma$-irradiation, the radiation induced crosslinking and degradation mechanism of the nanocomposites was proposed comprehensively.



Silicone rubber (SR) is a kind of polymer with the Si-O-Si backbone and organic groups attached to Si atom. Since Si-O bond has a higher dissociation energy compared with C–C bond [1], SR is more stable during lifetime than polyolefin. Therefore, it has a wide range of applications in extreme environment such as high temperature and high-energy radiation. However, how to make it more stable in such severe environment still needs to explore. Nowadays, many researches on modification of SR have been conducted, including physical mixing or chemical modification. The physical introduction of $SiO_2$ [2], carbon nanotube [3] or clays [4] can improve the performance of SR, while these fillers often tend to aggregate in some degree. Another remedy to modify SR is to form chemical bond between the fillers and SR, which often uses complicated synthesis route.

Polyhedral oligomeric silsesquioxane (POSS) is one new type of nano-hybrid organic-inorganic material with the typical formula $RSiO_{1.5}$. It is showed that organic substituents attached to the inorganic cage make POSS easier to mix with the polymer matrix. The incorporation of POSS into polymers can dramatically improve its mechanical properties [5,6], thermal stability [7,8], flame retardancy [9], radiation resistance [10–12], ionic conductivity [13,14] and dielectric properties [15]. Recently, there are some articles about POSS/SR nanocomposite, mainly focusing on mechanical property and thermal stability of the composites. Chen *et al.* synthesized novel POSS as cross-linkers to prepare novel POSS/SR nanocomposite with special three-dimensional structure [16], and they found the composites had significantly enhanced thermal stabilities, mechanical properties and hardness as compared to the SR prepared with the conventional cross-linkers. Bai *et al.* prepared chemical-modified liquid SR with octalvinyl POSS (Ov-POSS) by the hydrosilylation reaction [5], and the results showed that the thermal stability of POSS was improved. It is widely believed that chemical incorporation of POSS into the matrix have significant effect on the performance of SR. However, Xu *et al.* synthesized three kinds of POSS (aminopropyl, mercaptopropyl and chloropropyl) to physically mix with silicone resins by thermal curing [8]. They found that POSS can improve the performance of SR by physical blend.

In addition, previous studies have shown that POSS/polymer composites have better radiation resistance than the matrix due to

* Corresponding author.
*E-mail address:* mlzhai@pku.edu.cn (M. Zhai).
[1] These authors contributed equally to this work.

https://doi.org/10.1016/j.cclet.2022.03.068
1001-8417/

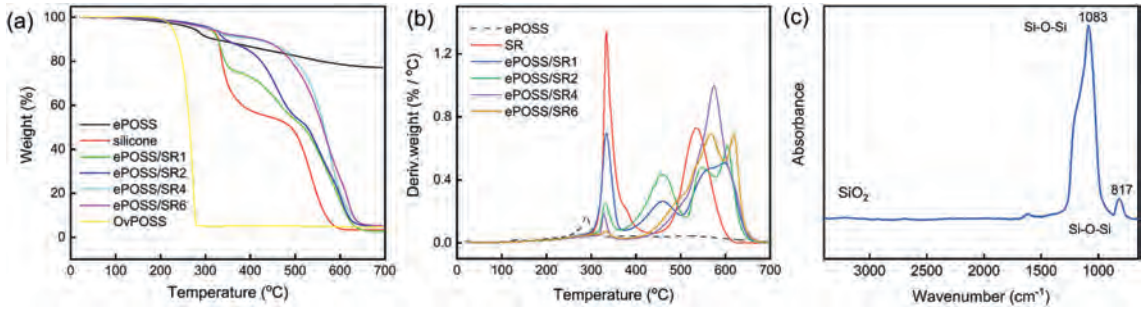


**Fig. 1.** (a) TG and (b) DTG thermograms of ePOSS, SR and ePOSS/SR nanocomposite in the nitrogen atmosphere; (c) FTIR spectra of the residue remaining after ePOSS was heated to 700 °C.

that the rigid inorganic core of POSS is not easy to be damaged under irradiation. Even at high dose, the inorganic core of POSS will turn to a dense and stable $SiO_2$ layer attached to the surface of the materials, protecting it from further degradation. For example, Qian *et al*. found that POSS/polyimide blends could resist atomic oxygen (AO) attack, which could be used as the outer surface material of spacecraft [10]. And Wang *et al*. prepared a kind of durable AO-resistant coatings that are capable of autonomously healing mechanical damage under low earth orbit environment [11]. This coating was comprised of 2-ureido-4[1*H*]-pyrimidinone functionalized polyhedral oligomeric silsesquioxane (UPy-POSS) that forms hydrogen-bonded three-dimensional supramolecular polymers. The preparation of high-performance SR nanocomposite with excellent radiation resistance is of great importance in engineering applications. However, there are few reports on the study of radiation resistance of POSS/SR nanocomposite.

In this work, to develop a simple remedy for improving the thermal property and radiation resistance of SR, epoxy-POSS (ePOSS) with better compatibility with SR was synthesized by oxidizing OvPOSS with *meta*-chloroperoxybenzoic acid, and characterized by FTIR, NMR and MS (synthesis and characterization of ePOSS as shown in Supporting information). Then ePOSS/SR nanocomposites were prepared by simple solution blending (experimental section in the supporting information). To explore the effects of ePOSS on the matrix, the cross-linking density, mechanical properties, thermal stability and radiation resistance were studied, respectively. Fig. 1a showed the TG thermograms of OvPOSS, ePOSS, SR and ePOSS/SR nanocomposites. Contributed to the stiff inorganic core, OvPOSS was very stable until the temperature reached 252 °C. Above 252 °C, OvPOSS powder began to sublimate [17]. Finally, only 5.3% residue remains at 278 °C. However, the oxidized ePOSS did not tend to sublime when heating in the nitrogen. That is, the thermal stability of ePOSS was higher than OvPOSS, and its highest weight loss rate existed at 289 °C (Fig. 1b). From Fig. 1c, it was found that the residue of ePOSS at 700 °C was $SiO_2$, and the actual residue was 77.1%. It is worth mentioning that the introduction of ePOSS significantly improved the thermal decomposition temperature of the SR matrix. Here we defined the temperature at the mass loss of 5% is $T_5$, same as $T_{10}$. As shown in Table S1 (Supporting information), $T_5$ increased from 310 °C of SR to 421 °C of ePOSS/SR6 nanocomposites, with about 34.8% growth. In addition, $T_{10}$ increased from 329 °C of SR to 484 °C of ePOSS/SR6 nanocomposites, with nearly 47.1% growth. It was reported that the thermal decomposition mechanism of SR consists of unzip degradation and rearrangement degradation [18]. In the unzip degradation stage, the terminal hydroxyl groups of SR would bite back into the main chain and cause unzip degradation. In the rearrangement decomposition reaction, the Si-O-Si backbone would be broken randomly, and rearrangement degradation occurs.

As shown in Fig. 1b, the first weight loss peak at 300 ~ 400 °C corresponding to the unzip decomposition stage gradually decreased and shifted to a higher temperature. When the content of ePOSS is 6 wt%, only a small peak remains in this decomposition stage, indicating that the unzip degradation reaction was almost inhibited by ePOSS. Resulting from the physical interaction between ePOSS and the SR matrix, the introduction of ePOSS significantly increased the thermal decomposition temperature of SR. In the related literature, Zhang *et al*. prepared vinyl-POSS-reinforced SR with chemical bond, and found the $\Delta T_5$ is only 18 °C when the content of vinyl-POSS is 6 wt% [19], the same content as in our work. And Xu *et al*. published an article on greatly improving thermal stability of silicone resins by modification with aminopropyl-POSS by forming hydrogen bond between aminopropyl-POSS and silicone resins [8], in which $\Delta T_5$ of the composite is 45 °C at the content of aminopropyl-POSS 1 wt%. However, aminopropyl-POSS begins to aggregate when the content continues to increase, and the thermal stability of the composites obviously decreases. In our work, ePOSS significantly improves the thermal stability of SR by simple physical mixing. ePOSS/SR6 nanocomposites had excellent properties and thermal stability, which was selected as the experimental sample of radiation resistance, and SR as the control sample. By comparison, the effect of fillers and absorbed doses on the properties of SR were explored. Finally, the radiation crosslinking and degradation mechanisms of ePOSS/SR nanocomposite were analyzed *via* structural characterization and measurement of radiolysis products. Fig. 2a compared the $v_{\text{e-total}}$ of SR and ePOSS/SR6 nanocomposites at different absorbed doses. With the increase of the absorbed dose, the $v_{\text{e-total}}$ of SR and ePOSS/SR6 nanocomposites gradually increased, and $v_{\text{e-chem}}$ of ePOSS/SR6 nanocomposites increased more obviously than that of SR. The higher absorbed dose was, the more free radicals generated in the polymer. Then the free radicals caused the crosslinking between the polymer chains, so the $v_{\text{e-total}}$ increased with the increasing absorbed dose. In addition, the side chain of ePOSS would react with the chain of the polymer under irradiation, leading to the higher growth of $v_{e\text{-}chem}$ of ePOSS/SR nanocomposite. And this phenomenon was similar to the previous studies on the effect of $SiO_2$ filler on SR radiation stability [20].

The surface functional groups of SR and ePOSS/SR6 nanocomposites at different absorbed doses were analyzed by ATR-FTIR (Fig. 2b). By comparison, it was found that the ATR-FTIR spectra of SR at different absorbed dose were consistent in those of ePOSS/SR nanocomposites, excepting that SR at 300 kGy and 500 kGy had new absorption vibration peaks at 3142 $cm^{-1}$ and 3050 $cm^{-1}$, which may be belonged to the absorption of hydroxyl group. However, no new absorption peaks appeared in the ePOSS/SR6 at 300 kGy and ePOSS/SR6 at 500 kGy, indicating the presence of ePOSS can slow down the oxidation process of the SR surface. The soluble substance from SR to ePOSS/SR6 nanocomposites with different absorbed dose in $CDCl_3$ were characterized by $^1H$ NMR. Compared with irradiated SR at different absorbed dose, all of the irradiated ePOSS/SR6 nanocomposite had characteristic peaks at 2.6 ~

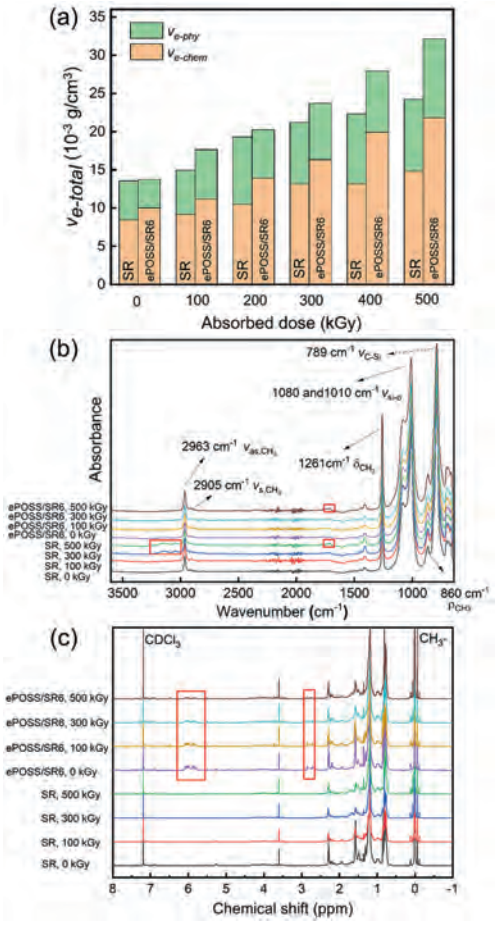


**Fig. 2.** In the air, the $v_e$ of SR and ePOSS/SR6 nanocomposites at different absorbed doses (a); ATR-FTIR spectra of SR and ePOSS/SR6 nanocomposites with different absorbed doses (b) and $^1$H NMR spectra of soluble substance from SR to ePOSS/SR6 nanocomposites dissolved in $CDCl_3$ before and after irradiation (c).

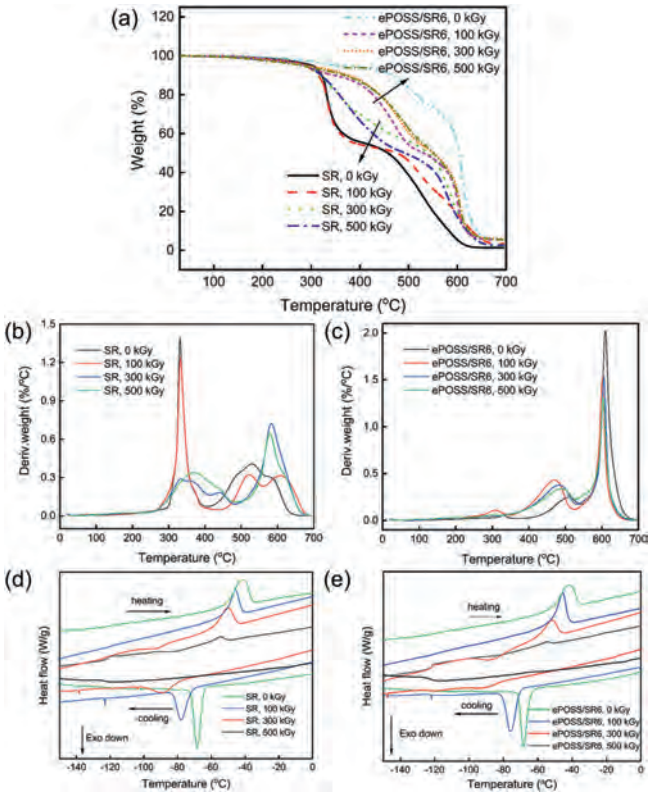


**Fig. 3.** TG (a) and DTG thermograms (b, c) of both SR and ePOSS/SR nanocomposite with different absorbed doses in the nitrogen atmosphere; DSC curves (d, e) of SR and ePOSS/SR nanocomposite with different absorbed doses in helium atmosphere.

2.9 ppm and 5.7∼6.1 ppm, which corresponded to the C–C bonds and epoxy bonds of ePOSS (Fig. 2c), respectively. That is, ePOSS would escape from the SR matrix and dissolve in $CDCl_3$ during the soaking process, which further proved that it was physically mixed in the SR matrix. However, as discussed about $v_{e\text{-}chem}$ above, chemical bonds formed between the reactive side chain of ePOSS and the matrix under irradiation. So these two characteristic peaks gradually became weaker with the increasing absorbed dose. In addition, no new characteristic peaks appeared in the spectra of SR and ePOSS/SR6 nanocomposites after 500 kGy, which means that no significant degradation of the samples occurred under this irradiation condition.

Fig. 3a showed the TG thermograms of both SR and ePOSS/SR6 under different absorbed doses. First, with the increasing absorbed dose, the thermal decomposition temperature of SR continued to improve due to the increasing crosslinking density. However, after $\gamma$-irradiation, the thermal decomposition temperature of irradiated ePOSS/SR6 nanocomposites were lower than that of the unirradiated sample. Subsequently, its thermal stability increased slightly with the increasing absorbed dose. It is possibly attributed to that under $\gamma$-ray irradiation, the physical interaction between ePOSS and the matrix was destroyed, leading to the reduction of thermal stability of the composites. At the same time, the chemical bond between ePOSS and the matrix formed, leading to a slight increase in thermal stability. By comparing Figs. 3b and c, it can be seen that the DTG curve of ePOSS/SR6 nanocomposites changed less than SR after irradiation, and its thermal stability was always higher than that of SR. As shown in Figs. 3d and e, the larger absorbed dose, the lower crystallization temperature ($T_c$), the lower melting temperature ($T_m$), the smaller $\Delta H_m$ and the lower crystallinity of the samples existed (Table S2 in Supporting information). In addition, the crystallization and melting peaks were rarely observed because of high $v_{e\text{-}total}$ of samples at the absorbed dose of 500 kGy. Considering what we have discussed above, with the increasing absorbed dose, the $v_{e\text{-}total}$ of the samples increased, making the polymer chain difficult to move. As the amorphous region of the sample increased, the crystallinity of the sample decreased and its crystallization and melting peaks move toward lower temperatures.

Due to the increasing $v_{e\text{-}total}$ of both SR and ePOSS/SR6 nanocomposites under irradiation, their tensile strength and elongation at break decreased, and Young's modulus increased (Figs. 4a–c). However, the rate of change in Young's modulus had distinct difference between irradiated SR and ePOSS/SR6 nanocomposites (Fig. 4d). During irradiation in the air, the oxygen would consume some free radicals of the samples, so their rate of changes rarely changed at the absorbed dose of 100 kGy. As the absorbed dose increasing, the oxygen in the air was not enough to consume all free radicals, and the left free radicals led to the chemical crosslinking inside the samples. Therefore, the Young's modulus of the samples gradually increased. When the rate of change of Young's modulus was 20%, the corresponding absorbed dose of SR and ePOSS/SR6 nanocomposite were 276.6 and 353.6 kGy, respectively. In general, the rate of change in Young's modulus of SR was always higher than that of ePOSS/SR6 nanocomposites, indicating the addition of ePOSS can improve the radiation resistance of SR. In addition, compared with irradiation in the air, both SR and ePOSS/SR6 nanocomposite had higher $v_{e\text{-}total}$ (especially $e_{v\text{-}chem}$) after irradiation in the nitrogen, which was consistent with previous studies [21]. Because

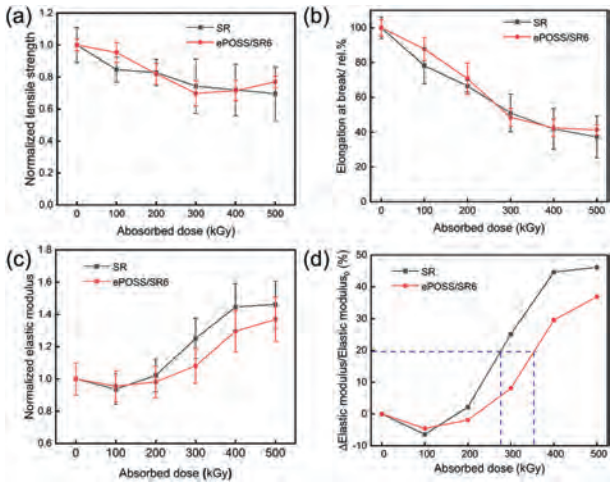


**Fig. 4.** Tensile strength (a), elongation at break (b), Young's modulus (c) and the rate of change in Young's modulus (d) of both SR and ePOSS/SR6 nanocomposites with different absorbed doses (in air).

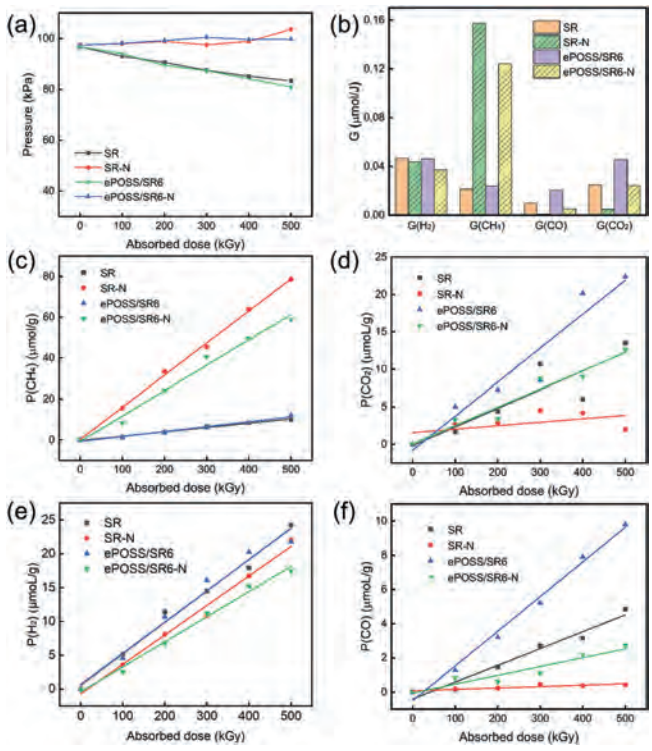


**Fig. 5.** (a) The pressure in the sample tube fitted with SR, SR-N, ePOSS/SR6 and ePOSS/SR6-N after irradiation with different absorbed doses; (b) G-value of $H_2$, $CH_4$, CO and $CO_2$ of SR, SR-N, ePOSS/SR6 and ePOSS/SR6-N; the output of $CH_4$ (c), $CO_2$ (d), $H_2$ (e) and CO (f) produced by SR, SR-N, ePOSS/SR6 and ePOSS/SR6-N after irradiation with different absorbed doses.

the free radicals generated by irradiation would not be consumed by oxygen under the protection of nitrogen.

Fig. 5a showed the pressure in the sample tube fitted with SR, SR-N, ePOSS/SR6 and ePOSS/SR6-N (N represents irradiation in the nitrogen) after irradiation with different absorbed doses. The pressure change of the sample tubes containing SR and ePOSS/SR composite had the same tendency whether samples were irradiated in the nitrogen or air. In the nitrogen, the pressure in the sample tube increased slightly with the increasing absorbed dose, indicating that samples produced some radiolysis gas after irradiation. However, the pressure in the sample tube decreased with

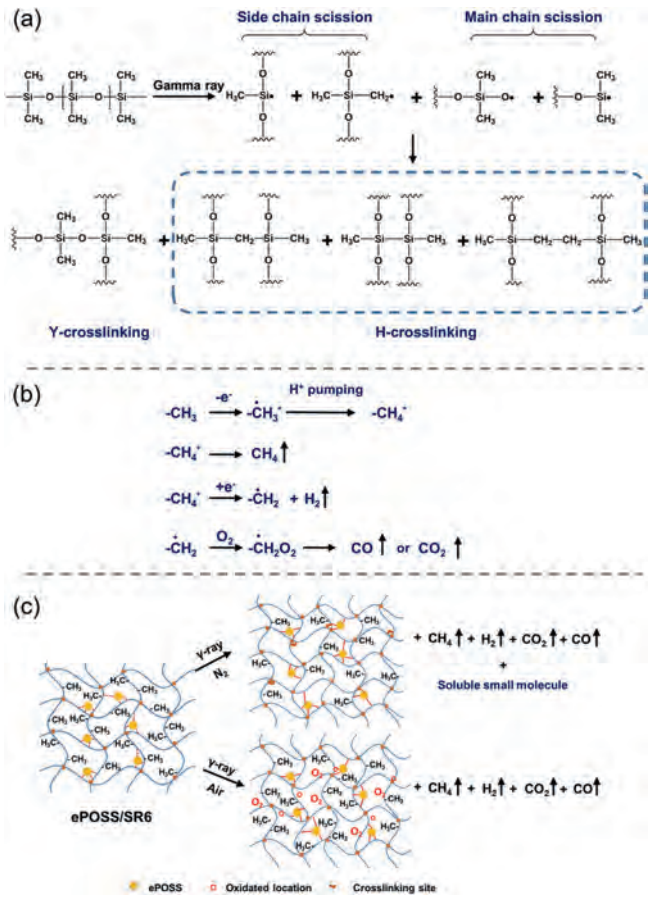


**Fig. 6.** (a) $\gamma$-Radiation induced crosslinking mechanism of PDMS; (b) The gas-releasing mechanism by the hydrogen pumping reaction of the methyl side chain of PDMS [27]. (c) The radiation induced crosslinking and degradation mechanism of ePOSS/SR6 at different atmosphere.

the increasing absorbed dose in the air, indicating that the oxygen participated in the reaction during the irradiation. Then GC was used to further detect the radiolysis gas generated during irradiation [22,23]. It was found the main gaseous radiolysis products of both irradiated SR and ePOSS/SR nanocomposite were $CH_4$, $CO_2$, $H_2$ and CO [23], whether irradiated in the air or nitrogen. As shown in Figs. 5c–f, the concentration ($P$) of these four gaseous radiolysis products increased with the increasing absorbed dose. Then the radiolysis gas yield ($G$) were calculated by linear fitting of relationship between the concentration of products with the dose (Fig. 5b and Table S3 in Supporting information). $G_{H_2}$ was independent of the irradiation atmosphere, but $G_{CH_4}$, $G_{CO_2}$ and $G_{CO}$ were greatly affected by the irradiation atmosphere. SR-N and ePOSS/SR-N had higher $G_{CH_4}$ and SR and ePOSS/SR had higher $G_{CO_2}$ and $G_{CO}$. The involvement of $G_2$ inhibited the cross-linking of SR-N and ePOSS/SR materials and suppressed the formation of $CH_4$. It indicates that oxygen is involved in the radiation degradation process of polymer chains. The change of $CH_4$ content is closely related to the environment in which the material is exposed to, so it is speculated that $CH_4$ can be used for the assessment of the radiation aging state of the material.

Based on the above analysis, the radiation induced cross-linking and degradation mechanism of ePOSS/SR nanocomposite were proposed in Fig. 6. The radiation crosslinking and degradation mechanism of PDMS under vacuum has been reported in literatures. Initially, Miller found that the methyl side chain of PDMS would break to generate -Si• and -$CH_2$• radicals to form H-type crosslinking during irradiation [21,24]. Then Hill *et al.* found that the main

chain Si-O-Si of PDMS would also break to generate free radicals to form Y-type crosslinking *via* recombination of Si-O bonds during irradiation, and Y-type crosslinking was the main type of the radiation crosslinking of PDMS (Fig. 6a) [25]. At the same time, the methyl side chain would also undergo a hydrogen pumping reaction to produce small molecular gasses such as $H_2$ and $CH_4$ during irradiation (Fig. 6b). If the samples were irradiated in the presence of oxygen, -Si• and -$CH_2$• radicals would be converted into their corresponding peroxy group [26] and would not directly participate in the H-type crosslinking reaction, but decompose to produce $CO_2$ and CO gas or form oxygen-containing groups on the surface of the material. In the nitrogen, the irradiated SR and ePOSS/SR6 nanocomposites mainly produced $CH_4$ and $H_2$, while the amount of CO and $CO_2$ was very small. However, ePOSS had eight organic side chains, which would be decomposed or oxidized. So $G_{CO_2}$ and $G_{CO}$ of ePOSS/SR6 nanocomposites were higher than these of SR. In the air, $G_{H_2}$ of ePOSS/SR nanocomposite was nearly same as that of SR, and its $G_{CH_4}$ slightly increased. However, its $G_{CO_2}$ and $G_{CO}$ significantly increased due to the presence of ePOSS. Fig. 6c shows the schematic diagram of the mechanism of ePOSS/SR6 during irradiation in the nitrogen or air. Thus, in this work, we suggested that with the increase of the absorbed dose, the more free radicals generated in SR and ePOSS/SR nanocomposite, the higher $v_{e\text{-total}}$ was, the harder the material became, and the better thermal stability was. As for as ePOSS/SR nanocomposite, ePOSS had physical interaction with SR matrix. While the physical interaction was broken and new chemical bonds between fillers and matrix formed in composites during irradiation. Finally, ePOSS acted as a crosslinking point or pendant in composites, which could improve the radiation stability of SR.

In summary, the radiation induced crosslinking and degradation mechanism of the ePOSS/SR nanocomposites under $\gamma$-irradiation was proposed comprehensively by analyzing the changes in the structure and properties of the materials and the radiolysis gasses (Fig. 6c), which provided the foundation for the application of this material in the nuclear radiation environment.

## Declaration of competing interest

The authors declare that they have no known competing financial interests or personal relationships that could have appeared to influence the work reported in this paper.

## Acknowledgments

This work was financially supported by the Science Challenge Project (No. TZ2018004) and the National Natural Science Foundation of China (NSFC, Nos. 11575009 and 12075010).

## Supplementary materials

Supplementary material associated with this article can be found, in the online version, at doi:10.1016/j.cclet.2022.03.068.

## References

[1] A. Charlesby, Nature 173 (1954) 679–680.
[2] J. Xie, J. Hu, X.D. Lin, et al., Appl. Surf. Sci. 457 (2018) 870–880.
[3] W.Q. Shen, R.N. Ma, A. Du, et al., Appl. Surf. Sci. 447 (2018) 894–901.
[4] Y.T. Zhu, R. Cardinaels, J. Mewis, P. Moldenaers, Rheol. Acta 48 (2009) 1049–1058.
[5] H.Q. Bai, C. Huang, L. Jun, H.B. Li, J. Appl. Polym. Sci. 133 (2016) 43906.
[6] F. Wang, Y.D. Wu, Y.D. Huang, L. Liu, Compos. Sci. Technol. 156 (2018) 269–275.
[7] H.D. Liu, G.M. Zhu, C.S. Zhang, Compos. Part B 190 (2020) 107901.
[8] Y.Y. Xu, J. Long, R.Z. Zhang, et al., Polym. Degrad. Stab. 174 (2020) 109082.
[9] W.J. Zhang, G. Camino, R.J. Yang, Prog. Polym. Sci. 67 (2017) 77–125.
[10] M. Qian, V.J. Murray, W. Wei, B.C. Marshall, T.K. Minton, ACS Appl. Mater. Interfaces 8 (2016) 33982–33992.
[11] X.H. Wang, Y.X. Li, Y.H. Qian, et al., Adv. Mater. 30 (2018) 1803854.
[12] L. Yu, S. Liu, B. Liu, et al., Polym. Degrad. Stab. 198 (2022) 109893.
[13] J.F. Zhang, C. Ma, J.T. Liu, et al., J. Membr Sci. 509 (2016) 138–148.
[14] W.J. Na, A.S. Lee, J.H. Lee, et al., Solid State Ion. 309 (2017) 27–32.
[15] P.S. Zong, J.F. Fu, L.Y. Chen, et al., RSC Adv. 6 (2016) 10498–10506.
[16] D.Z. Chen, S.P. Yi, W.B. Wu, et al., Polymer 51 (2010) 3867–3878.
[17] M.N. Shi, T.R. Lin, Y. Hu, et al., J. Mater. Sci. 55 (2020) 1489–1498.
[18] T.S. Radhakrishnan, J. Appl. Polym. Sci. 73 (1999) 441–450.
[19] Y. Zhang, Y.W. Li, J. Zheng, et al., J. Appl. Polym. Sci. 132 (2015) 42187.
[20] A. Chien, R. Maxwell, D. Chambers, B. Balazs, J. LeMay, Radiat. Phys. Chem. 59 (2000) 493–500.
[21] A.A. Miller, J. Am. Chem. Soc. 83 (1961) 31–36.
[22] B. Liu, P.C. Wang, Y.Y. Ao, et al., Radiat. Phys. Chem. 133 (2017) 31–36.
[23] B. Liu, W. Huang, Y.Y. Ao, et al., Polym. Degrad. Stab. 147 (2018) 97–102.
[24] A.A. Miller, J. Am. Chem. Soc. 82 (1960) 3519–3523.
[25] D.J.T. Hill, C.M.L. Preston, D.J. Salisbury, A.K. Whittaker, Radiat. Phys. Chem. 62 (2001) 11–17.
[26] L.E. Stpierre, H.A. Dewhurst, J. Phys. Chem. 64 (1960) 1060–1062.
[27] H. Menhofer, H. Heusinger, Radiat. Phys. Chem. 29 (1987) 243–251.